SIMULATION OF A HIGH-FLUX RISER-REACTOR FLOW USING CFD TECHNIQUES

Leonardo Machado da Rosa, University of Campinas, Campinas, SP, Brazil
Jaci Carlo Schramm Camara Bastos, University of Campinas, Campinas, SP, Brazil
Milton Mori, University of Campinas, Campinas, SP, Brazil
Waldir Pedro Martignoni, Cenpes/Petrobras, Rio de Janeiro, RJ, Brazil

Abstract

The application of Computational Fluid Dynamics (CFD) in industrial operations has been increased not only in the project of new equipments but also in the optimization of the existing ones. The present work shows a set of three-dimensional two-phase and adiabatic conditions, using the two-fluids model for the calculation of gas-solids flow in a high-flux risers of two different geometries, one with 10m of height and 76mm of internal diameter, and the second with 18m of height and 50mm of internal diameter. The k-epsilon model was applied to consider the influence of turbulence over the gas phase. The four-lump and ten-lump schemes kinetic models were used to predict the catalytic cracking reactions in the two different reactors. The first riser had two entrances, one for particles and one for the organic materials. The mesh size for this case was 584,000 control volumes. The second studied riser had one entrance for vapor, one for organic materials, and a third for particles. The mesh generated over this geometry had 650,000 control volumes. The numerical results of gas-solids dispersion flow in a high-flux were compared with the experimental data from the work of Pärssinen and Zhu [8], the four lump scheme for the mass concentration of chemical species was compared with the work of Ali *et al*. [2], and the ten lump scheme was compared with the work of Nayak *et al*. [7]. The catalytic cracking reactions models show an important role in the prediction of all phenomena present in the reactor. The simulated results show that the kinetics models are important not only because of the variation of the gas phase and the temperature profiles inside the reactor but also because these parameters interfere directly in the dynamic behavior of the gas-solid flows.

KEYWORDS: CFD, gas-solid, catalytic cracking

Introduction

A fluidized catalytic cracking unit (FCCU) consists of a riser reactor, where the catalytic reactions occur, and a regenerator, where the catalyst is reactivated. The main purpose of the riser is to put into contact hydrocarbons and catalyst particles, causing the catalytic cracking reactions. The cracking process converts the hydrocarbons fed into products with a higher commercial value. Although this equipment is widely used, phenomena in risers have not yet been entirely explained. They are operated with a high concentration of particles in a fluidized bed regime (fast transport regime). The adoption of fluidized beds is related to the catalytic cracking of gasoil in gasoline; previously, cracking had been done in fixed bed reactors.

Multiphase flows are more difficult to predict and analyze because their phases can assume complicated configurations [3, 5]. The phases do not mix uniformly and interactions between the phases (on a small scale) can have a strong effect on the macroscopic properties of the flow. The formation of heterogeneous structures in gas-particle systems (e.g., clusters) strongly affects the gas-

solid contact and transport processes in dense fluidized beds. These structures depend on the overall forces acting on the particles. The drag force plays a fundamental role in the coupling of gas and particles. Zhang and Reese [9] propose a new equation for the mean drag force that considers not only the solids volumetric fraction, but also random fluctuations in particle movement.

In the modeling of chemical reactions, the use of groups of chemical species (or *lumps*) is common. A lump is the representation of a group of chemical species that have similar chemical properties. Thus, the catalytic cracking reactions that occur concurrently between numerous chemical species can be modeled as reactions between a fewer number of lumps [4]. The advantage of this procedure is the small number of chemical species and of reaction rates that have to be calculated separately, requiring a data bank for their calculation, and proportional computational resources. In the literature simulations that apply lumps to model the catalytic cracking of hydrocarbons, in gas-solid reaction systems [1, 2], or three-phase systems [7] are mainly one-dimensional. However, one-dimensional simulations cannot provide realistic solutions for radial distributions and are not able to properly handle some phenomena, such as particle reflux and swirls in a turbulent flow, and one-dimensional balances cannot be applied at the entrance region due to the high nonhomogeneity and turbulence in this region.

This article shows the influence of cracking models on the fluid flow through simulations with and without calculating reactions and with different cracking models. The finite volume method was utilized.

Mathematical Modeling

For simulation of the flow inside the reactor, the flow of two phases was considered: the particulate phase, consisting of catalyst particles, and the gaseous phase, a mixture of water vapor and organic compounds. The formation of new products and consumption of the existing ones alter the physicochemical properties of the gaseous phase. Both phases are fed at different temperatures; thus, at the bottom of the reactor, high temperature gradients exist.

Gas-solid systems can be modeled by several techniques. One consists in modeling each phase separately with the established equations for one-phase flows with a moving surface between them. However, when the phases are well mixed, as in many industrial operations, these cases require an average procedure to make the solution of the equations possible.

Ishii [6] divides the models for solution of fluid flow problems into two categories: diffusion models and two-fluid models. A diffusion model is formulated considering the mixture to have one transport equation for the continuity, momentum and energy, and a diffusion equation. A two-fluid model consists in two equations for the continuity, momentum and energy, one for each phase. In this work, the Eulerian-Eulerian approach was also applied. The *k-epsilon* model was applied to take account of the turbulent behavior of the flow. The equations of the model are given below.

Momentum and Continuity Conservation Equations

The continuity conservation transient equations for each phase (gas and particulate solids) are as follow:

$$\frac{\partial}{\partial t}\left(\varepsilon_g \rho_g\right)+\nabla\cdot\left(\varepsilon_g \rho_g u_g\right)=0 \tag{1}$$

$$\frac{\partial}{\partial t}\left(\varepsilon_p \rho_p\right)+\nabla\cdot\left(\varepsilon_p \rho_p u_p\right)=0 \tag{2}$$

where ε_g and ε_s are the volume fractions, ρ_g and ρ_s are the density of both phases, gas and particulate solids respectively; *u* is the velocity vector, and S_i^ρ represents the source term of continuity for each phase. The right hand side of the Equations 1 and 2 are null, due to the assumption of no mass transfer between phases. The momentum conservation equations are as follow:

$$\frac{\partial}{\partial t}\left(\varepsilon_g \rho_g u_g\right)+\nabla\cdot\left(\varepsilon_g \rho_g u_g u_g\right)=-\varepsilon_g \nabla p_g+\nabla\left(\varepsilon_g \mu_g\left(\nabla u_g+\left(\nabla u_g\right)^T\right)\right)+\varepsilon_g \rho_g g+\beta_{gp}^m\left(u_p-u_g\right) \quad (3)$$

$$\frac{\partial}{\partial t}\left(\varepsilon_p \rho_p u_p\right)+\nabla\cdot\left(\varepsilon_p \rho_p u_p u_p\right)=-G\nabla \varepsilon_p+\nabla\left(\varepsilon_p \mu_p\left(\nabla u_p+\left(\nabla u_p\right)^T\right)\right)+\varepsilon_p \rho_p g+\beta_{pg}^m\left(u_g-u_p\right) \quad (4)$$

where μ is the viscosity. *G* represents the elasticity modulus, β^m the momentum transfer coefficient, and *g* the gravity vector.

Chemical Species Transport

The concentration of the chemical species are calculated with another transport equation given in Equation 5:

$$\frac{\partial}{\partial t}\left(\varepsilon_g \rho_g c_i\right)+\nabla\cdot\left(\varepsilon_g \rho_g u_g c_i\right)=\nabla\left(\varepsilon_g \Gamma_i \nabla c_i\right)+S_g^i \quad (5)$$

where S_g^i represents the formation or consumption of each specie.

Energy Transport

$$\frac{\partial}{\partial t}\left(\varepsilon_g \rho_g H_g\right)+\nabla\cdot\left(\varepsilon_g \rho_g u_g H_g\right)=\nabla\left(\varepsilon_g \lambda_g \nabla T_g\right)+\beta_{gp}^h\left(T_p-T_g\right)+\sum_r \Delta H\frac{\partial c_r}{\partial t} \quad (6)$$

$$\frac{\partial}{\partial t}\left(\varepsilon_p \rho_p H_p\right)+\nabla\cdot\left(\varepsilon_p \rho_p u_p H_p\right)=\nabla\left(\varepsilon_p \lambda_p \nabla T_p\right)+\beta_{pg}^h\left(T_g-T_p\right) \quad (7)$$

Closure Equations

The term $G\nabla\varepsilon_p$ in Equation 4 is a simple model for the adjustment of the solids pressure (fluidized bed case), which is related to all other spatial directions. The convenient form to express *G* is given by Equation 8:

$$G=\exp\left(600\left(\varepsilon-0.62\right)\right) \quad (8)$$

The coefficients of friction or drag between fluid and particles are obtained from standard correlations with the negligence of acceleration. The momentum transfer coefficient between gas phase and particles is in accordance with Equation 9:

$$\beta_{gp}^m=\frac{3}{4}\mathrm{Cd}\frac{\left|u_p-u_g\right|\varepsilon_p \rho_p}{d_p}f\left(\varepsilon\right) \quad (9)$$

where the *f* is the volume fraction correction, $f = \varepsilon^{-1.65}$. The drag coefficient, *Cd*, applied to Equation 9, is a function of the Reynolds number and behaves (for $Re_p < 1000$) according to

$$Cd = \frac{24}{Re}\left(1 + 0.15 Re^{0.687}\right) \tag{10}$$

or (for nonlaminar flows, with $Re_p > 1000$)

$$Cd = 0.44 \tag{11}$$

For dense flows (i.e., when $\varepsilon_p > 0.2$), the momentum transfer coefficient between gas and particles is

$$\beta_{gp}^{m} = 150\frac{\varepsilon_p^2 \mu_g}{\varepsilon_g d_p^2} + 1.75\frac{|u_p - u_g|\varepsilon_p \rho_p}{d_p} \tag{12}$$

For the calculation of the heat transferred between phases, the Nusselt number obtained from the Ranz-Marshall model is used:

$$Nu = 2 + 0.6 Re_p^{1/2} Pr^{1/3} \tag{14}$$

In Equation 6, the formation and consumption of chemical species are considered at the last term of the equation. The reactions can behave as a 2nd order kinetic model (Equation 15) or as a 1st order kinetic model:

$$\frac{\partial c_r}{\partial t} = -k_r \varepsilon_s c_i^2 \tag{15}$$

$$\frac{\partial c_r}{\partial t} = -k_r \varepsilon_s c_i \tag{16}$$

The k term in Equations 15 and 16 is adjusted with an Arrhenius equation,

$$k_r = k_0 \exp\left(\frac{-E_r}{RT}\right) \tag{17}$$

Chemical Kinetic Models

Several models are being proposed for the calculation of catalytic cracking reactions. The advances in both the analytical techniques and mathematical routines for determining the parameters lead to the progression from simple models with three and four lumps, to more complex models with ten, twelve, and more lumps.

The four-lump kinetic model classifies the hydrocarbon fractions into four groups, as illustrated in Figure 1. Oil cracking follows a second-order kinetics, while gasoline cracking follows a first-order

kinetics. Parameters for the determination of reaction rates and heat were found in the work of Ali *et al*. [2].

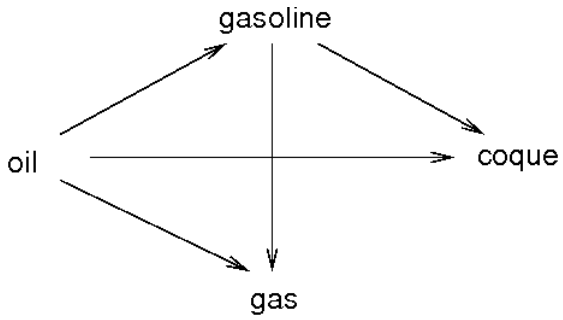

Figure 1. Four lumps kinetic model

Analogously, the ten-lump model describes the relationship of ten groups of hydrocarbons – four light hydrocarbon groups (paraffins, naphthenics, aromatics and aromatic substituents groups), four heavy hydrocarbon groups, coque and gasoline (Figure 2). Parameters for the determination of reaction rates and heat were found in the work of Nayak *et al*. [7].

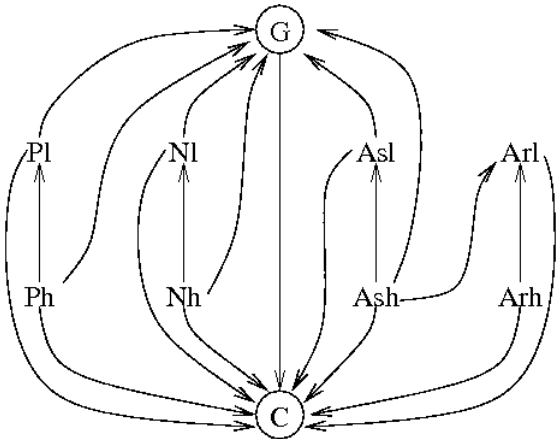

Figure 2. Ten lumps kinetic model

Meshes

Several three-dimensional mesh tests using hexahedral control volumes were elaborated for two different geometries. For all test cases a first control volume (at the walls) thickness of about 1mm, which provided the required value of y+ for the turbulence model. The first geometry, shown in Figure 3a, had a height of 10m and an internal diameter of 76mm, and was based on the equipment presented by Pärssinen and Zhu [8]. It is a combination of a cylindrical duct with a lateral junction that has the purpose of injecting the catalyst, and ends in a curve. A generation of mesh known as “O-Grid” was applied for the generation of a higher quality mesh. Meshes of different sizes were tested, and the mesh composed of 584,000 control volumes was chosen.

The second geometry, shown in Figure 3b, has a height of 18m and an internal diameter of 50mm. It is also a combination of a cylindrical duct with a lateral junction, and terminates with another junction that forms a 90 degrees angle with the main duct. It has two more entrances inside the reactor

for vapor and feed inlet. Because of the complexity of this geometry an "L-Grid" generation of mesh was applied in the curved inlet. The final mesh chosen for the second geometry was composed of 650,000 control volumes.

The generated meshes for each of the geometries are detailed in Figures 4 and 5, where it can be seen the distribution of the control volumes at (a) the inlet region, (b) the outlet region, and (c) a transversal section. A more refined grid was applied near the walls, and at the locations where strong gradients of both momentum and temperature exist.

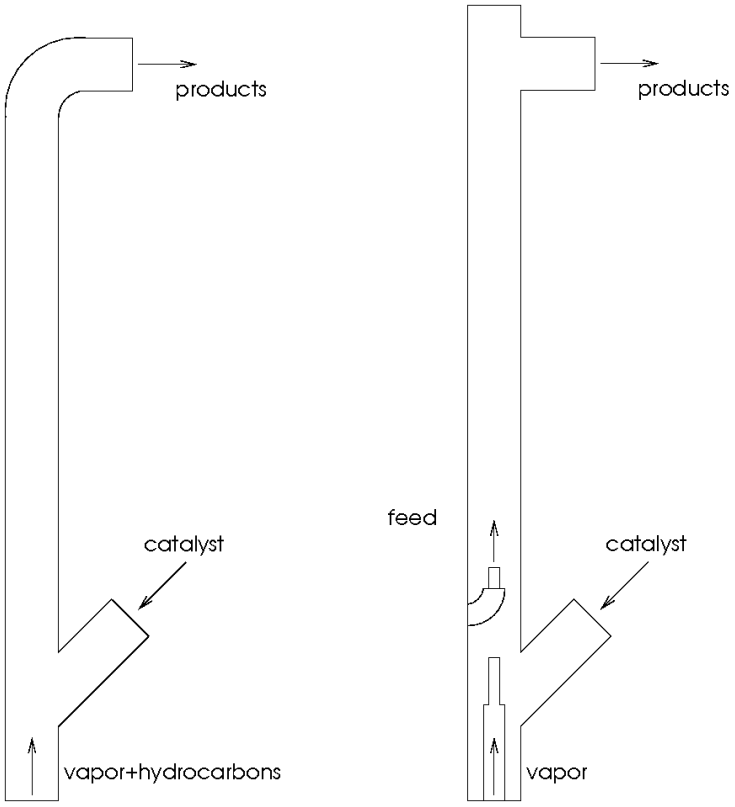

Figure 3. Geometries utilized

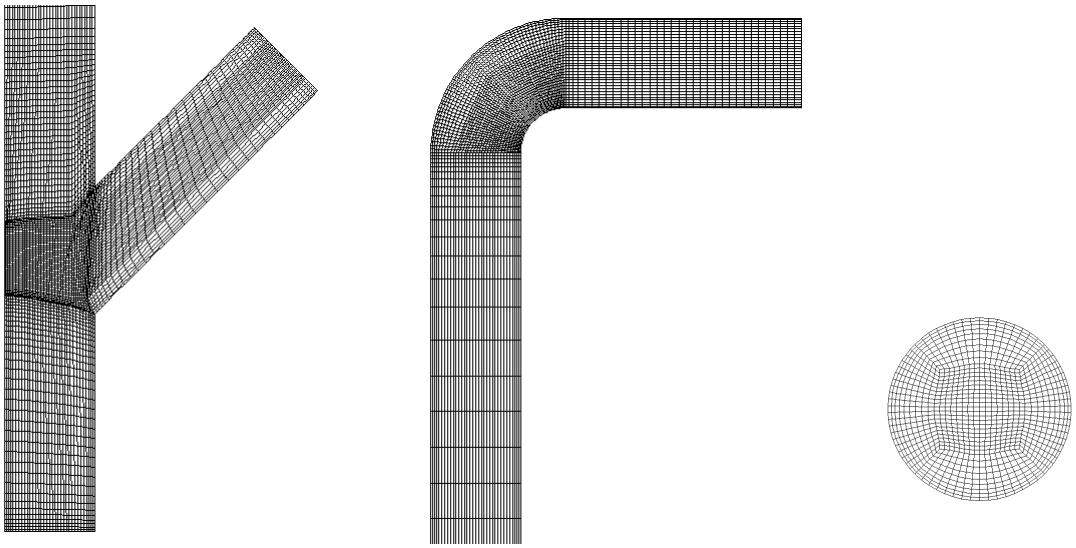

(a) (b) (c)

Figure 4. Mesh details for Geometry A

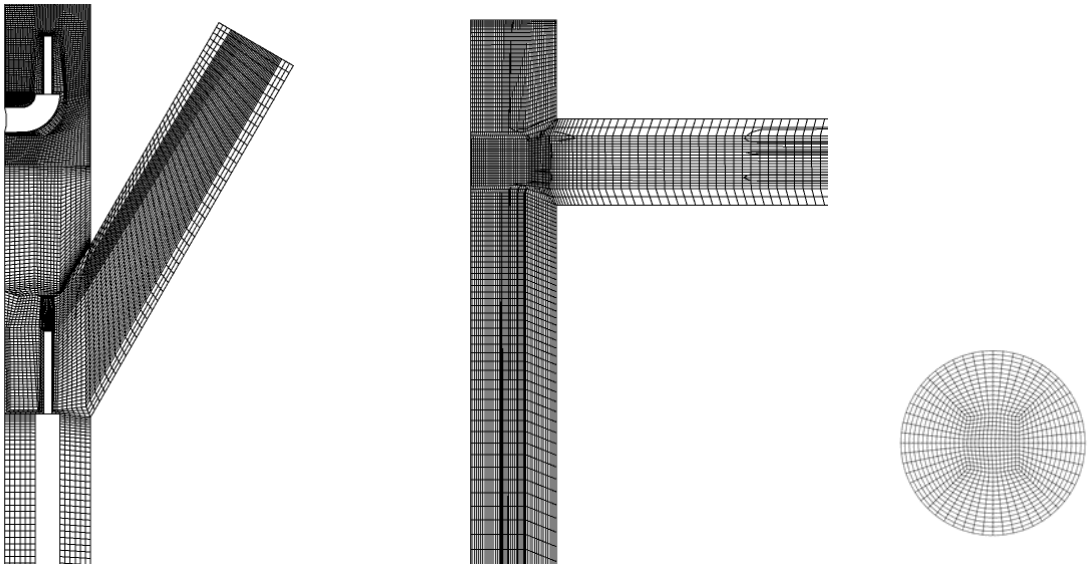

(a) (b) (c)

Figure 5. Mesh details for Geometry B

Results and Discussion

The following results were obtained with the simulation of a gas-solid system flowing at 5s. An initial time step of 0.0001s was used. The fluid considered in the simulations was a mixture of water vapor, air and hydrocarbons, with its physical properties varying with its composition. The particulate phase was a 1500 kg/m³ catalyst with a diameter of 67µm.

Figure 6 shows the gas-phase temperature maps calculated for the two geometries. In both cases it could be seen that these values are influenced by the temperature of the particle phase. In Figure 6a, more heat is transferred to the gas phase, whereas the temperature after the contact with hot catalysts is higher than the temperature in Figure 6b.

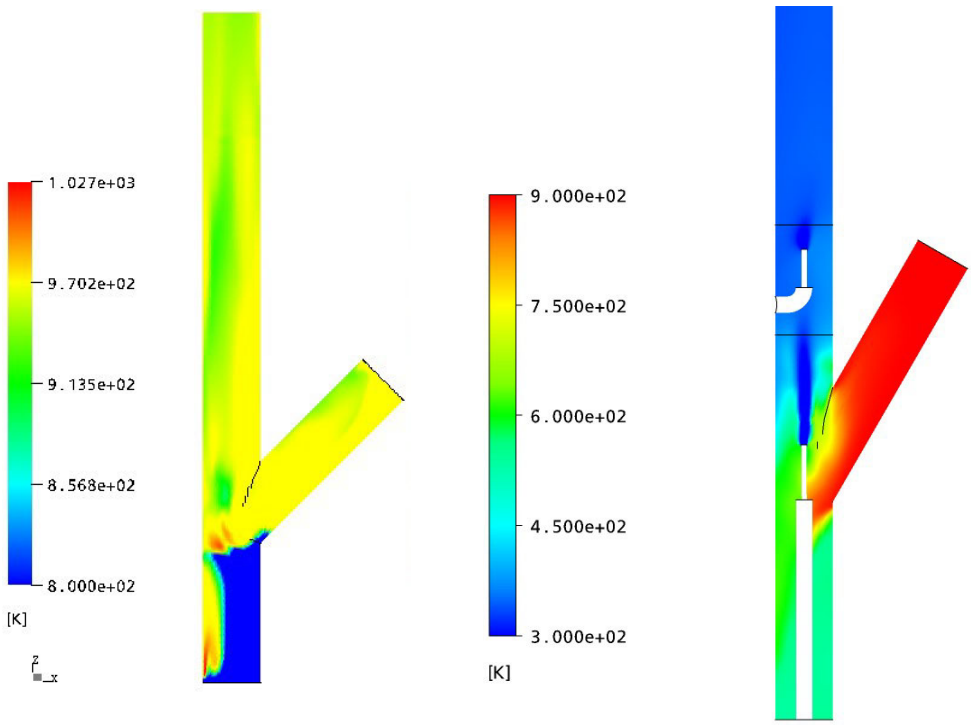

(a) (b)

Figure 6. Temperature maps along axial plane

Figure 7 shows the concentration profile of hydrocarbons calculated with the four-lump model for geometry A. The values obtained follow the same trends as the experimental ones (given by Ali *et al*. [2]), but the conversion was a little lower than expected. One possible explanation for this behavior could be the heat transfer model in which the chemical reactions are greatly influenced by the temperature.

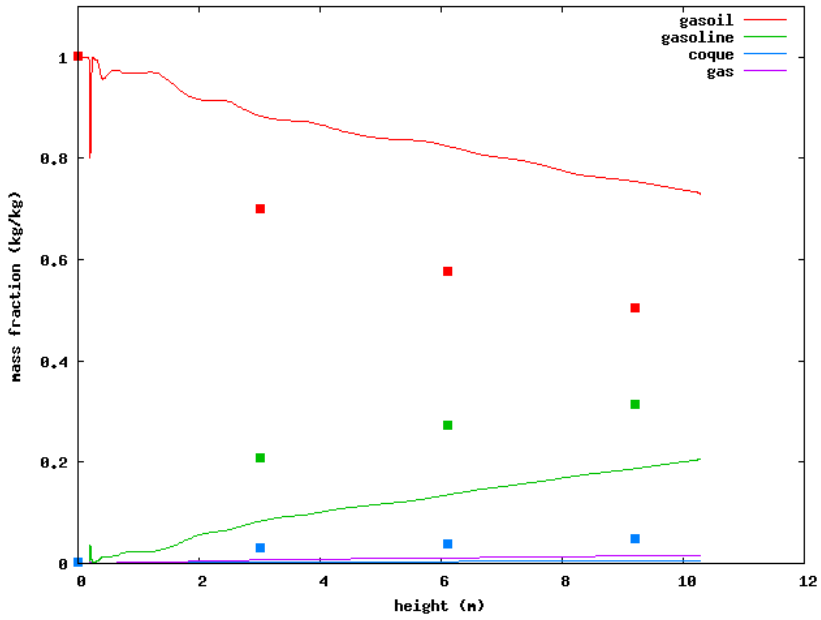

Figure 7. Hydrocarbons conversion along the axis

The behavior of the flow with reaction compared with the flow without reaction are shown in Figures 8 and 9. When the composition of the gas phase varies, its properties are not the same because they depend on the properties of each chemical species. Figure 8 shows the flow in the lower section of the reactor at a height of 1.53m. There are few differences between the profiles, but these are greater at higher heights (Figure 9) because there are more products formed in this region.

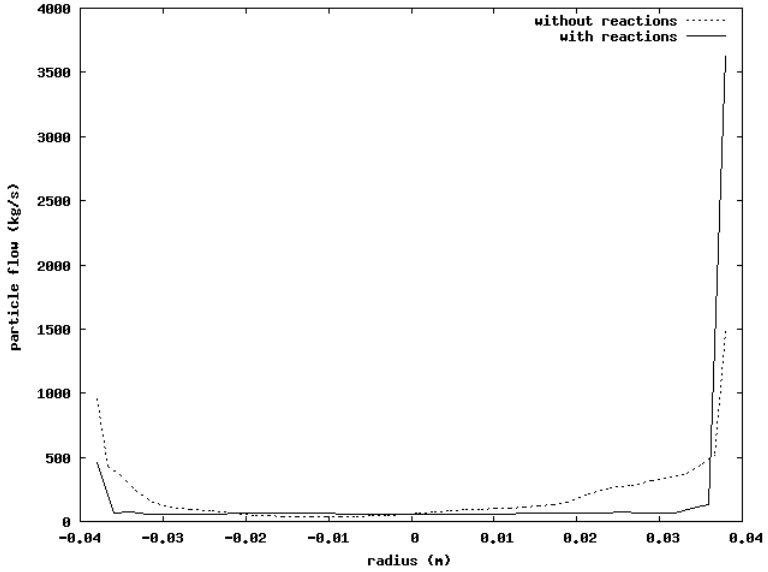

Figure 8. Comparison of flows at a height of 1.53m

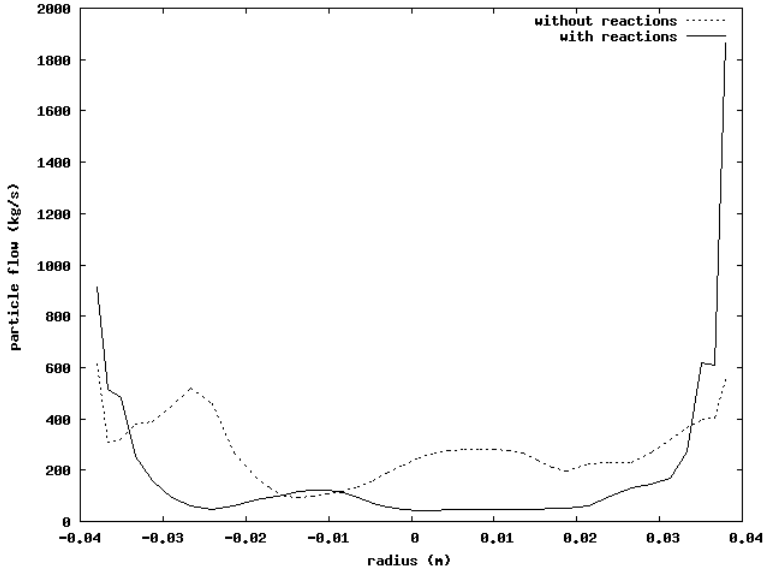

Figure 9. Comparison of flows at a height of 9.42m

Conclusions

The simulation of a reacting gas-solid fluid flow, coupling the four-lumps and ten-lumps kinetic models with the two-fluids model, was calculated for two different riser configurations in the CFX

package. Simulation of the reacting flows resulted in conversions lower than what was expected, but with the same trends. Further researches are in progress to extend this work to other heat transfer coefficients and more accurate analysis for the fluid dynamics of the flow at high temperatures. Results with and without chemical reactions showed differences, indicating the need of coupling these phenomena, even when comparing just the simulated fluid-dynamic with experimental data.

Acknowledgments

The authors would like to thank FAPESP and PETROBRAS for their financial support.

Nomenclature

c	species concentration	[kgmol/m³]
Cd	drag coefficient	[–]
d_p	particle diameter	[m]
E	activation energy	[J/mol]
g	gravity	[m/s²]
G	elasticity modulus	[Pa]
H	enthalpy	[J/kg]
k	reaction rate coefficient	[s-¹]
Nu	Nusselt number	[–]
P	pressure	[Pa]
R	gas universal constant	[J/(mol.K)]
Re	Reynolds number	[–]
Pr	Prandtl number	[–]
S	species source	
t	time	[s]
T	temperature	[k]
u	velocity	[m/s]
β	interphase transfer coefficient	[kg/(m²s)]
ε	volumetric fraction	[–]
λ	thermal conductivity	[W/(m.K)]
Γ	diffusivity	
μ	viscosity	[kg/(m.s)]
ρ	density	[kg/m³]

References

1. Ali, H., Rohani, S. (1997), "Dynamic modeling and simulation of a riser-type fluid catalytic cracking unit," *Chem. Eng. Technol.*, n. 20, pp. 118-130.
2. Ali, H., Rohani, S., Corriou, J.P. (1997), "Modelling and Control of a riser type fluid catalytic cracking (FCC) unit," *Trans. IchemE.*, 75A, pp. 401-412.
3. Bastos, J.C.S.C., Rosa, L.M., Mori, M., Marini, F., Martignoni, W.P. (2008), "Modelling and Simulation of a gas-solids dispersion flow in a high-flux circulating fluidized bed (HFCFB) riser," *Catalysis Today*, n. 130, pp. 462-470.

4. Farkas, G. (1999), "Kinetic lumping schemes," *Chemical Engineering Science*, 54, pp. 3909-3915.
5. Hanratty, T.J., Theofanous, T., Delhaye, J.M., Eaton, J., McLaughlin, Prosperetti, A., Sundaresan, S., Tryggvason, G. (2003), "Workshop findings," *International Journal of Multiphase Flow*, n. 29, pp. 1047-1059.
6. Ishii, M. (1975), *Thermo-Fluid Dynamic Theory of Two-Phase Flow*. Eyrolles.
7. Nayak, S.V., Joshi, S.L., Ranade, V.V. (2005), "Modeling of vaporisation and cracking of liquid oil injected in a gas-solid riser," *Chemical Engineering Science*, n. 69, pp. 6049-6066.
8. Pärssinen, J.H. and Zhu, J.X. (2001), "Particle velocity and flow development in a long and high-flux circulating fluidized bed riser," *Chemical Engineering Science*, 56, pp. 5295-5303.
9. Zhang, Y., Reese, J.M. (2003), "The drag force in two-fluid models of gas-solid flows," *Chemical Engineering Science*, v. 58, pp. 1641-1644.